

RESEARCH ARTICLE | NOVEMBER 10 2022

## Numerical simulations of a toroidal droplet breakup in viscous oils

Shiyi Qin; Zhaolin Li; Xun Wang; ... et. al



AIP Advances 12, 115213 (2022)

<https://doi.org/10.1063/5.0123867>View  
OnlineExport  
Citation

CrossMark

### Articles You May Be Interested In

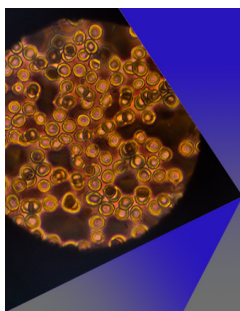
Viscoplastic toroidal drop in compressional Stokes flow

*Physics of Fluids* (July 2021)

Modeling of drop breakup in the bag breakup regime

*Appl. Phys. Lett.* (April 2014)

Effect of airflow pressure on the droplet breakup in the shear breakup regime

*Physics of Fluids* (May 2021)

## AIP Advances

Special Topic: Medical Applications  
of Nanoscience and Nanotechnology

**Submit Today!**

# Numerical simulations of a toroidal droplet breakup in viscous oils

Cite as: AIP Advances 12, 115213 (2022); doi: 10.1063/5.0123867  
Submitted: 1 September 2022 • Accepted: 14 October 2022 •  
Published Online: 10 November 2022



View Online



Export Citation



CrossMark

Shiyi Qin,<sup>1</sup> Zhaolin Li,<sup>1</sup> Xun Wang,<sup>2</sup> Kai Li,<sup>3,a)</sup> and Xue Chen<sup>1,b)</sup> 

## AFFILIATIONS

<sup>1</sup>School of Mechanical and Electrical Engineering, Guilin University of Electronic Technology, Guilin 541004, China

<sup>2</sup>School of Reliability and Systems Engineering, Beihang University, Xueyuan Road No. 37, Haidian District, Beijing 100083, China

<sup>3</sup>National Microgravity Laboratory, Institute of Mechanics, Chinese Academy of Sciences, Beijing 100190, China

<sup>a)</sup>Also at: School of Engineering Science, University of Chinese Academy of Sciences, Beijing 100149, China.

<sup>b)</sup>Also at: Guangxi Key Laboratory of Manufacturing System and Advanced Manufacturing Technology, Guilin University of Electronic Technology, Guilin 541004, China. **Author to whom correspondence should be addressed:** [chenxue@guet.edu.cn](mailto:chenxue@guet.edu.cn)

## ABSTRACT

Toroidal droplets are inherently unstable in viscous oils; they either shrink to a single drop or break into several spherical droplets due to Rayleigh–Plateau instability. In this paper, the breakup dynamics of toroidal droplets in immiscible viscous oils have been numerically investigated. A two-dimensional model combined level-set method is proposed. Numerical results reveal that the initial aspect ratios, interfacial tensions, and outer liquid viscosities play important roles in determining the breakup dynamics of toroidal droplets. The initial aspect ratios dominate the number of split droplets, which is consistent with a linearly scaling law  $n = 0.57 R_0/a_0$ . By considering key factors of interfacial tension in this process, it is found that interfacial tension is crucial in the initial morphology of the toroidal droplet and helps to retard the unstable breakup dynamics. Interestingly, reducing the interfacial tension stabilizes it against breakup. We further study the effect of viscosity on the breakup dynamics. The surrounding viscous oils contribute to stabilizing the interfacial-tension-driven instabilities and extending the breakup time. Thus, for a toroidal droplet in high viscosity oils and a sufficiently low interfacial tension system, the unstable breakup dynamics could be delayed. Our findings provide a novel fundamental understanding of toroidal droplets and are beneficial to applications involving the manipulation of toroidal droplets.

© 2022 Author(s). All article content, except where otherwise noted, is licensed under a Creative Commons Attribution (CC BY) license (<http://creativecommons.org/licenses/by/4.0/>). <https://doi.org/10.1063/5.0123867>

## I. INTRODUCTION

Toroidal droplet is inherently unstable in immiscible viscous oils due to their nonminimal surface shapes. Driven by surface tension, the unstable morphologies tend to a perfectly spherical shape to minimize the surface area for a given volume.<sup>1–3</sup> The rich dynamics of toroidal droplets in viscous oils are ubiquitous in nature, such as falling raindrops, underwater ring bubbles, biofilms, and self-assemble copper rings.<sup>4–7</sup> Among the above-mentioned applications, forming a stable torus in an immiscible phase and resisting their morphologies deformation in the absence of external fields remain a big challenge; for instance, in the three-dimensional (3D) bioprinting process, maintaining the initial shape relatively stable and retarding the original deformation time in an aqueous two-phase system are essential for forming desired 3D architectures in

the rapid curing stage.<sup>8</sup> Indeed, it is common to generate toroidal droplets by injecting fluids within a rotating container filled with another immiscible liquid.<sup>9,10</sup> Then, the challenge still exists in controlling the dynamic evolutions of an initially unstable morphology of the torus. Therefore, it is of great importance to understand the dynamics of a toroidal droplet in viscous oils to manipulate their on-demand breakup for various applications.

When a toroidal droplet was suspended in a viscous phase, two distinct phenomena depending on the aspect ratio were experimentally demonstrated.<sup>11</sup> For thin torus, it breaks into several spherical droplets through the capillary driven by Rayleigh–Plateau instability. If the torus is sufficiently fat, it shrinks toward the center to form a single droplet due to shrinking instability. Motivated by the experiments of Páram and Fernández-Nieves,<sup>11</sup> many theoretical

and numerical models have been performed, implying that the presence of viscous stress and surface stress dominated the evolution process.<sup>12–17</sup> Zhao and Tao<sup>18</sup> developed a theoretical model of a liquid ring in a gas medium, and the weakly nonlinear instability indicated that surface tension, an external force from ambient fluid, and viscosity significantly affected the breakup dynamics. Mehrabian and Feng<sup>19</sup> established a Cahn–Hilliard diffuse-interface model to compute the capillary breakup. They found that toroidal droplets rupture depended on the competition of two-time scales, i.e., torus retraction and neck pinch-off. The final breakup pattern was determined by the initial amplitude of the disturbance, initial aspect ratio, and torus-to-medium viscosity ratio. The previous models<sup>19–21</sup> mainly focused on the linear and nonlinear stability analyses and discussed the variation of the growth rate or growth disturbance, which were difficult to measure in the experiments. However, the dominant factors of aspect ratio and breakup time on the breakup dynamics are still inadequately understood. Thus, the stabilization of toroidal droplets by controlling the interfacial tension and viscosities of outer phases needs to be investigated exclusively.

In this work, we propose a two-dimensional (2D) model to simulate the breakup dynamics of toroidal droplets in immiscible viscous oils numerically. The effects of initial aspect ratios, interfacial tensions, and outer liquid viscosities are systematically studied. The initial aspect ratios dominate the number of split droplets, which is consistent with a linearly scaling law. Interestingly, we find that the toroidal droplets with a low interfacial tension system are different from those with high interfacial tension systems. It suggests that interfacial tension plays a significant role in initial morphology, and low interfacial tension stabilizes it against breakup. We further investigate the effect of viscosity on the breakup dynamics, indicating that surrounding viscous oils contribute to stabilizing the surface-tension-driven instability and extending the breakup time. Our results provide important missing pieces to enrich the fundamental understanding of toroidal droplets in a variety of viscous systems and could be beneficial for applications involving the manipulation of toroidal droplets.

## II. MATERIALS AND METHODS

### A. Problem statement

In the experiments, a toroidal droplet is formed by injecting inner liquids into a rotating bath containing immiscible viscous oils, as shown schematically in Fig. 1. A container ( $d = 36$  mm) filled with silicon oil ( $\rho_o = 963$  kg/m<sup>3</sup>) is located on the top of the rotating stage (Zolix, China), which drives the container to rotate at the same angular speed. The inner liquid of glycerol ( $\rho_i = 1252$  kg/m<sup>3</sup> and  $\mu_i = 945$  mPa·s) is pumped into the viscous oil by a syringe pump (Longer Pump, China) through a metallic needle ( $d_{out} = 1.08$  mm and  $d_{in} = 0.72$  mm). The flow rate  $q$  is controlled at 50 ml/h, and then, the volume of the toroidal droplet is mainly determined by the injection time  $t_i$ ,  $V_i = q \cdot t_i$ . As for a torus, the volume is equal to  $V_i = 2\pi^2 a_0^2 R_0$ , where  $a_0$  is the radius of its cross-section and  $R_0$  is the distance from the needle to the rotation axis, as shown in Fig. 2. By changing the location of the needle and the torus volume, the forming torus with different initial aspect ratios  $R_0/a_0$  is obtained. To investigate the effects of interfacial tension on droplet breakup, the surfactant Tween 20 of different mass ratios is added to the inner liquid of glycerol. The interfacial tension between glycerol solution

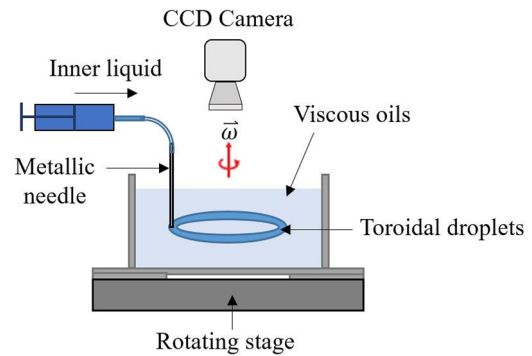


FIG. 1. Schematic of the experiment apparatus of a toroidal droplet in viscous oils.

and silicon oil is measured by the Pendant drop method.<sup>22</sup> By adding 0.5%, 1.5%, and 2% Tween 20, the measured interfacial tensions are different from the pure glycerol of 27 mN/m, changing to 16, 14, and 13 mN/m, respectively. For exploring the influence of the viscosity, silicon oils with different viscosities of 10 000, 30 000, and 60 000 mPa·s are used as the outer phase. After the toroidal droplet is generated, the time-dependent evolutions of the toroidal droplet breakup by the Rayleigh–Plateau instability are recorded with a high-speed camera at 170 fps.<sup>23</sup> The corresponding aspect ratio is analyzed by open-source software Image J. The uncertainties in the measurement method due to the single-pixel scaling and the selection of the contour are estimated to be  $\pm 0.08$  mm.

### B. Numerical model

In the numerical simulations, we consider a millimeter-sized toroidal droplet suspending in immiscible viscous oils with a confined wetted wall. A transient 2D model from the top view of the experiments is proposed, and the torus interface on the symmetric mid-plane is illustrated in Fig. 2. The middle torus represents the domain of glycerol solution; the rest parts represent the outer silicone oils. Thus, the immiscible two-phase border is the interface boundary. It is assumed that the two immiscible liquid phases

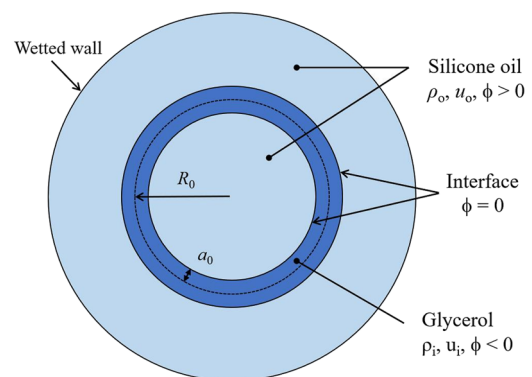


FIG. 2. Schematic of the numerical model and boundary conditions.

are incompressible viscous laminar flow, and the physical properties are constant. In addition, the effects of gravity and buoyancy are neglected.

The proposed model consists of the interaction of two immiscible liquid phases and their flow characteristics. The governing continuity equation and incompressible Navier–Stokes equations are

$$\nabla \cdot \mathbf{u} = 0, \tag{1}$$

$$\rho \left( \frac{\partial \mathbf{u}}{\partial t} + \mathbf{u} \cdot \nabla \mathbf{u} \right) = \nabla \cdot (-p\mathbf{I} + \mu \cdot \nabla \mathbf{u}) + \mathbf{F}_{st}, \tag{2}$$

where  $\rho$ ,  $u$ ,  $p$ ,  $I$ , and  $\mu$  stand for the density, velocity, pressure, tensor operator, and dynamical viscosity, respectively.  $\mathbf{F}_{st}$  represents the surface force.

To accurately capture the evolutions of the free interfaces between glycerol and immiscible silicone oil, a level-set method is proposed. The interface dynamics of the two liquid phases can be tracked by solving the transport equation of the level-set function  $\Phi$  due to the underlying physical velocity field. The function  $\Phi$  is governed by

$$\frac{\partial \Phi}{\partial t} + \mathbf{u} \cdot \nabla \Phi = \alpha \nabla \cdot \left( \varepsilon_s \nabla \Phi - \Phi(1 - \Phi) \frac{\nabla \Phi}{|\nabla \Phi|} \right), \tag{3}$$

where  $\Phi$  is the level-set function. It should be noted that  $\Phi = 1$ ,  $\Phi = 0$ , and  $\Phi = 0.5$  represent the domain of glycerol, silicone oil, and the sharp two-phase interface, respectively.  $\alpha$  is the reinitialization parameter, and  $\varepsilon_s$  is the controlling parameter of interface thickness.

Thus, the surface tension force at the interface is given by

$$\mathbf{F}_{st} = \nabla \cdot (\sigma(\mathbf{I} - (\mathbf{n}_{int} \mathbf{n}_{int}^T))\delta), \tag{4}$$

where  $\mathbf{n}_{int}$  is the unit normal vector perpendicular to the free interface,  $\sigma$  is the interfacial tension, and  $\delta$  a non-zero Dirac-delta function only at the fluid interface. The unit normal vector  $\mathbf{n}_{int}$  and Dirac-delta function are calculated by

$$\mathbf{n}_{int} = \frac{\nabla \Phi}{|\nabla \Phi|}, \tag{5}$$

$$\delta = 6 |\Phi(1 - \Phi)| |\nabla \Phi|. \tag{6}$$

The density and viscosity of the inner and outer phases are discontinuous but can be continuously calculated from the level-set function  $\Phi$ ,

$$\rho = \rho_o + (\rho_i - \rho_o)\Phi, \tag{7}$$

$$\mu = \mu_o + (\mu_i - \mu_o)\Phi. \tag{8}$$

Here, the subscript  $o$  represents the outer phase of silicon oils, and  $i$  denotes the inner liquid of glycerol.

The domain size is chosen as the container dimension, so the outer boundary is set as the wetted wall, considering non-slippery and no mass penetration, which denotes

$$\mathbf{u} \cdot \mathbf{n}_{wall} = 0. \tag{9}$$

Since the numerical model is an unsteady problem, initial conditions are also prescribed. At  $t = 0$ ,  $\Phi$  has to be initiated. Setting  $\Phi = 1$  is the glycerol and  $\Phi = 0$  is the silicon oils. Then, a toroidal droplet with differing initial aspect ratios  $R_0/a_0$  forms in viscous oils. The two-phase flow is at rest ( $\mathbf{u} = 0$ ); the initial pressure and temperature of the whole domain are set to be zero and ambient temperature, respectively.

### C. Numerical simulation validation

The commercial software COMSOL Multiphysics v5.6 is used to solve the laminar two-phase flow problem. By using the level-set method, the interface can be precisely tracked, and the final breakup patterns are obtained.<sup>24,25</sup> For spatial and temporal discretization of the finite element method, the P2+P1 is adopted, which means the velocity components are second-order and the pressure components are first-order. We conduct the transient fully coupled solution method, while the backward Euler formula is used for the nonlinear solution and the backward difference formula is utilized in the linear solution. The maximum relative tolerance on the dependent variable ( $\mathbf{u}$ ,  $p$ ) is lower than 0.1% during the iterative process.

To assess the accuracy of the numerical simulations, a grid sensitivity analysis has been first undertaken. We generate a free triangle mesh in the computational domain. The detail of the generated mesh is displayed in Fig. 3. Mesh refinement is conducted at the interface boundary. After several numerical experiments, grids with a total quantity of 20 532 elements are selected to control the relative error within 1%.

To validate the accuracy of the numerical simulations, we calculate the breakup behaviors of the toroidal droplet. According to the experimental results in Ref. 11, we build a 2D model with an aspect ratio of  $R_0/a_0 = 12.3$ . Glycerol and silicon oil are chosen as the two immiscible liquid phases, and then, the interfacial tension is 4 mN/m. Figure 4 displays the comparisons of the numerical results and experimental results at the initial state, before the breakup, and final state, resulting in multiple spherical droplets. We find that when the toroidal droplet is inserted into the viscous oil [Fig. 4(a1)], it may undergo a long time to reach the most unstable state due to the experimental disturbance as Fig. 4(a2), and then, it breaks into six small droplets, so the time from the beginning to the end of break is 14 s. However, in the simulations, the toroidal droplet breaks quickly; thus, it needs about 12 s from the beginning to the end of the break. We can conclude that the predictions of the toroidal droplet breakup from the 2D numerical simulations closely match

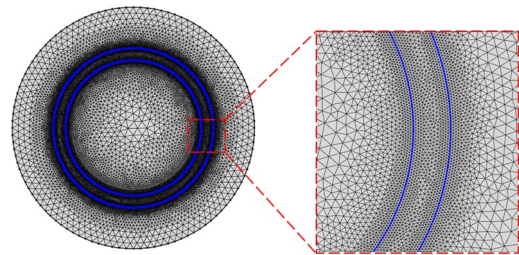
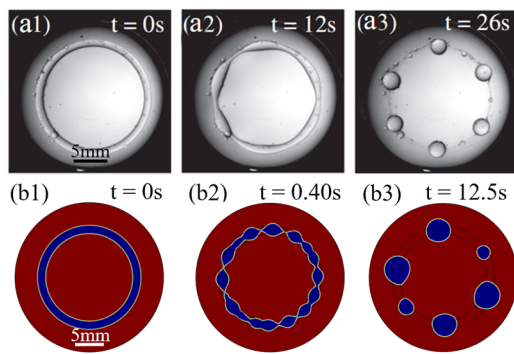


FIG. 3. The details of the generated mesh and its refinement at the interface boundary.



**FIG. 4.** Comparison of the breakup behaviors of a glycerol toroidal droplet in silicone oil. (a) Experimental results, reprinted with permission from E. Pairam and A. Fernández-Nieves, *Phys. Rev. Lett.* **102**(23), 234501 (2009). Copyright 2009 American Physical Society. (b) Numerical results ( $R_0/a_0 = 12.3$ ,  $\sigma = 4$  mN/m, and  $\mu_i/\mu_o = 1/30$ ). The two black circles in (b2) and (b3) represent the initial state of the toroidal droplet in the numerical simulation.

the 3D dynamic results in the experiments, which further proves the effectiveness of the proposed 2D model and meshing.

### III. RESULTS AND DISCUSSION

It should be noted that a toroidal droplet suspended in viscous oils is in an unstable state and tends to minimize its surface area due to interfacial tension. Under the surface force driven, it shrinks to form a single drop or breaks into several spherical droplets due to the Rayleigh–Plateau instability, which mainly depends on its initial aspect ratio. Furthermore, the viscosity of the outer phase also plays a significant role in the breakup dynamics. Therefore, numerical simulations are conducted for different initial aspect ratios, interfacial tensions, and outer liquid viscosities. In addition, the following experimental data from the literature<sup>23</sup> used for comparison with numerical results are all our previous work. Then, the corresponding results and discussions are presented in the following sections.

#### A. Effects of initial aspect ratios on the breakup dynamics

To investigate the dynamic evolutions from the formation to shrinkage/breakup process, toroidal droplets with different initial aspect ratios are calculated. In this study, the working fluid of the inner and outer phases are glycerol and silicone oil, the viscosity ratio is 0.03, and the interfacial tension is 27 mN/m. Figure 5 shows the numerical results of toroidal droplets with initial aspect ratios ranging from 2.5 to 22. It is found that two distinct mechanisms of shrinkage and breakup instabilities arise. In the first column of Fig. 5, when the initial aspect ratio is  $R_0/a_0 = 2.5$ , the liquid toroidal droplet shrinks toward its center and eventually coalesces into a single droplet. This shrinkage instability is always present with a small initial aspect ratio. However, the other columns in Fig. 5 exhibit breakup instability, which becomes the dominant mechanism for the initial aspect ratio to be larger than 5. In this case, only unstable modes with a wavelength consistent with the torus length can grow, and then, it breaks into several spherical droplets. More importantly, the number of droplets that split increases from two to eight

droplets corresponding to the initial aspect ratio. The numerical results also reveal that for an initial aspect ratio of 12.2, the final breakup pattern forms five spherical droplets at the breakup time  $t = 21.8$  s.

For obtaining a quantitative result of the breakup instability, the number of split droplets  $n$  as a function of the aspect ratio  $\xi = R_0/a_0$  is plotted in Fig. 6. For the numerical results, the aspect ratio for each simulation is measured from the beginning to the state of being broken up. According to our experimental observation, the toroidal droplets often shrink before it breaks up where the aspect ratio decreases. The rightmost open symbol in Fig. 6 represents the initial aspect ratio, and the leftmost open symbol indicates the growth rate corresponding to the fastest unstable mode. Such breakup instability of toroidal droplets is determined by the wavelength, which are integer fractions of the overall length of the torus that can induce its breakup:  $2\pi R_0 = n\lambda$ . Here,  $\lambda$  is the wavelength associated with the fastest unstable mode that dominates the breakup behaviors, and  $n$  is the number of split droplets. We obtained a linearly scaling law  $n = 0.57R_0/a_0$  in the previous experiments<sup>23</sup> and plotted it as the dashed line in Fig. 6. The derived numerical results suggest that the aspect ratio at the fastest unstable mode is linear with the number of split droplets, which is in good agreement with the previous experimental results. When the torus is very large, the breakup dynamics yield the liquid jet instabilities. A jet always breaks into drops due to the Rayleigh–Plateau instability. Linear stability analysis is used to understand how these perturbations lead to jet breakup. Remarkably, the classical stability analysis of Tomotika<sup>26</sup> for a viscous, cylindrical jet inside another viscous liquid predicts that the unstable mode with the largest growth rate corresponds to  $n = 0.54 R_0/a_0$ ; this value agrees with our numerical results.

#### B. Effect of interfacial tension on the breakup dynamics

To elucidate the underlying mechanism of interfacial tension on the breakup dynamics, a series of numerical simulations are carried out. In the numerical simulations, we keep the viscosity ratio constant ( $\mu_i/\mu_o = 0.03$ ), but the interfacial tensions and corresponding initial aspect ratios are determined by the initial conditions in our experiments.<sup>23</sup> Under the differing interfacial tension, the toroidal droplets will be stable under different initial conditions, resulting in various initial aspect ratios. Specifically, the initial conditions depend on whether the toroidal droplet could be formed as a closed ring. Here, there exists a rotational velocity  $v_0$ , if the velocity is not large enough, then the liquid jet will break before the torus is formed. This suggests that the relevant time scales are balancing with the time for forming a torus ( $t_1 = 2\pi/\omega = 2\pi R_0/v_0$ ) and rupturing a curved jet ( $t_2 = \mu_o d_{in}/\sigma$ ). Thus, to form a closed torus, the velocity reaches a critical value, which can be deduced by  $v_0 = (2\pi/\mu_o)(R_0/a_{tip})\sigma$ . We assume that  $R_0/a_{tip}$  approximates the aspect ratio, so the interfacial tension is inversely related to the aspect ratio, which means low interfacial tension corresponds to a large initial aspect ratio.

Figure 7 displays the temporal evolutions of the aspect ratio  $\xi$  with respect to non-dimensional time ( $t^* = t/t_{max}$ ) under different interfacial tensions. The measured aspect ratios from the numerical simulations are plotted as filled symbols, and the shape of the toroidal droplets at the initial and the final states are also shown in

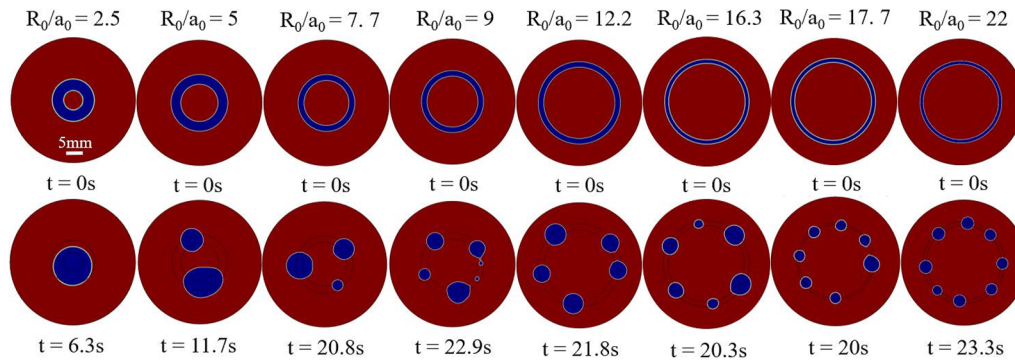


**FIG. 5.** Numerical results of toroidal droplets in viscous oils at different initial aspect ratios. The scale bar corresponds to 5 mm. The counter of the inner phase is glycerol, and the outer phase is silicon oil ( $\sigma = 27 \text{ mN/m}$ ,  $\mu_i/\mu_o = 0.03$ ). The two black circles in the second line represent the initial state of the toroidal droplet in the numerical simulation.

Fig. 7. At  $t^* = 0$ , when  $\sigma = 13 \text{ mN/m}$ , the initial aspect ratio is  $R_0/a_0 = 16.2$ , and when  $\sigma = 14 \text{ mN/m}$ , the initial aspect ratio is  $R_0/a_0 = 14.7$ , while  $\sigma = 16 \text{ mN/m}$ , the initial aspect ratio is 13.1. After the toroidal droplet is formed in the viscous oils, it shrinks gradually and the aspect ratio decreases with time. When the  $t^* > 0.7$ , the aspect ratio keeps almost constant and lasts until the end of the breakup process, leading to a relatively stable state. For the effect of interfacial tension, although the initial aspect ratio is different, the final aspect ratio is all around 6 and splits into six spherical droplets.

It should be noted that the whole breakup process will last longer in a low interfacial tension system. To further study the underlying mechanisms, we focus on the relationship between non-dimensional breakup time and interfacial tension, as shown in Fig. 8. The interfacial tensions are varied from 13 to 27 mN/m. The dashed line indicates the numerical results, and the filled symbols represent the experimental results.<sup>23</sup> As the interfacial tension increases, the breakup time of toroidal droplets decreases, which means that

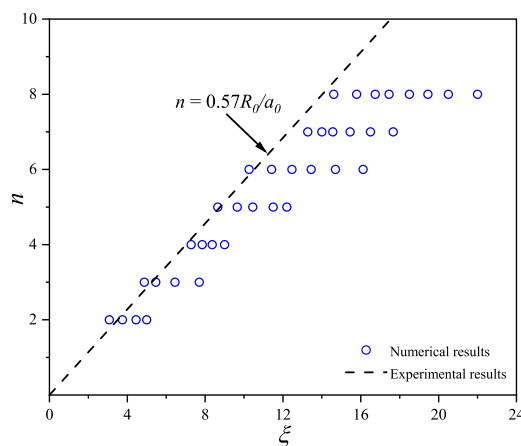


**FIG. 6.** The phase diagram of the number of split droplets is a function of the aspect ratio. The open symbols represent the numerical results from the beginning to the state of being broken up. The dashed line indicates the experimental results in the literature.

reducing the interfacial tension could stabilize it against breakup. The reason can be illustrated by the classical hydrodynamic instability of a liquid jet, where the breakup time is defined:  $t_2 = \mu_o d_{in}/\sigma$ .<sup>11</sup> It can be seen that the breakup time can be well fitted by an inverse law with  $t^* = 15.37\sigma^{-1}$ . Therefore, the low interfacial tension between two immiscible phases plays a crucial role in the initial morphology of the toroidal droplet and helps to retard the unstable breakup dynamics.

### C. Effect of viscosity on the breakup dynamics

The existing hydrodynamic instability theory also suggests the dependence of the viscosity on the breakup dynamics. In this section, silicone oils with different viscosity ( $\mu_o = 10\,000, 30\,000, \text{ and } 60\,000 \text{ mPa}\cdot\text{s}$ ) were used and kept the glycerol viscosity constant. The interfacial tension is set to be 13 mN/m, and the initial aspect ratios are constant at 16.3. Figure 9 displays the temporal evolutions of the aspect ratio  $\xi$  with respect to non-dimensional time ( $t^* = t/t_{\text{max}}$ )

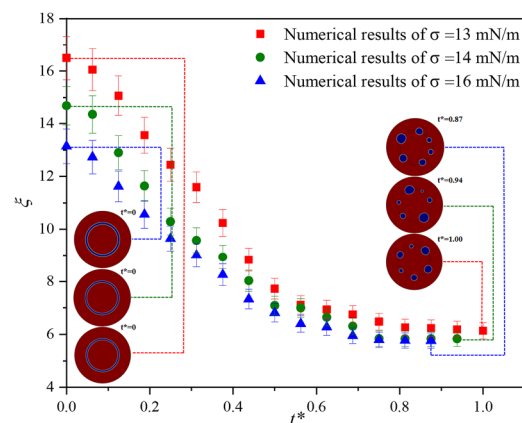


**FIG. 7.** Temporal evolutions of the aspect ratio with respect to non-dimensional time under different interfacial tensions. The red, green, and blue symbols stand for interfacial tensions of 13, 14, and 16 mN/m, respectively. Contours are the shapes of the toroidal droplets from the numerical simulations.

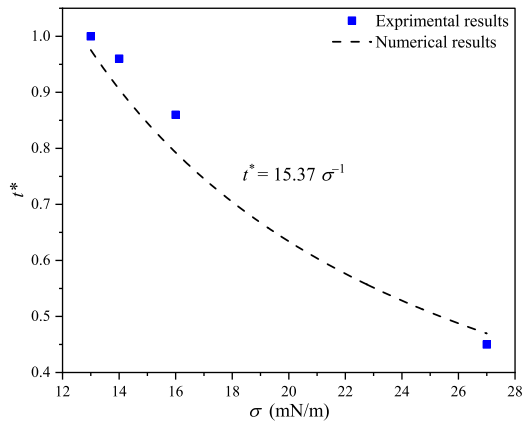


**FIG. 8.** The relationship between non-dimensional breakup time and interfacial tension. The dashed line indicates the numerical results, and the filled symbols represent the experimental results.

under different viscosities. We find that the viscosity of the outer phase greatly affects the breakup dynamics, but the final breakup pattern looks the same, exhibiting six spherical droplets. For a highly viscous system, i.e.,  $\mu_o = 60\,000$  mPa·s, the toroidal droplet slowly shrinks and reaches a constant aspect ratio of around 6. On the contrary, in a less viscous system of 10 000 mPa·s, the breakup behavior occurs in a short time, and the aspect ratio is about 6. The reason can be illustrated as follows: when a liquid is injected into a rotating viscous phase, the viscous oils drag the outer phase exerts over the injected liquid, and two relevant stresses are balanced in the process. The interfacial stress offers the driving force to shrink, and the viscous stress opposes the shrinkage process. The competition between these two stresses results in a breakup phenomenon. As a result, viscous stress helps to stable the interfacial-tension-driven instabilities and extend the breakup time.

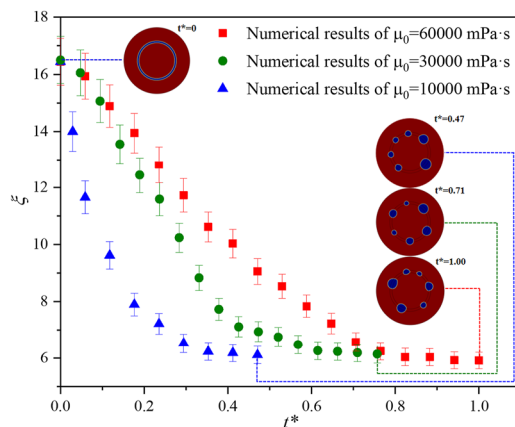


**FIG. 9.** Temporal evolutions of the aspect ratio with respect to non-dimensional time under different viscosity of silicon oil. The blue, green, and red symbols stand for viscosities of 10 000, 30 000, and 60 000 mPa·s, respectively. ( $\sigma = 13$  mN/m and  $R_0/a_0 = 16.3$ ) Contours are the shapes of the toroidal droplets from the numerical simulations.

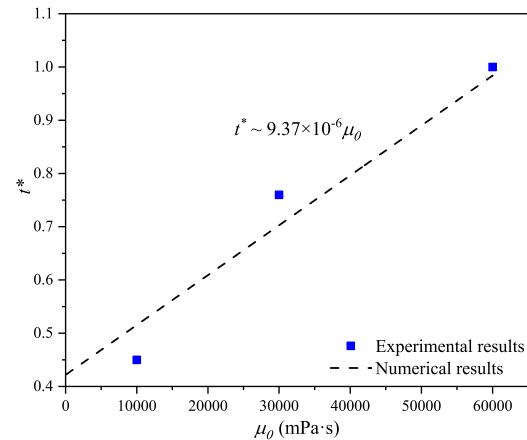


**FIG. 10.** The relationship between non-dimensional breakup time and outer phase viscosity. The dashed line indicates the numerical results, and the filled symbols represent the experimental results.

Obviously, the breakup time of toroidal droplets in various viscous oils is considerably different. Such a breakup process in a highly viscous system becomes slower. The relationship between non-dimensional breakup time and outer phase viscosity is shown in Fig. 10. The outer phase viscosities are ranging from 10 000 to 60 000 mPa·s. The filled symbols denote our experimental results obtained,<sup>23</sup> while the dashed lines correspond to numerical results. We find that the breakup time for the viscous oil with 10 000 mPa·s is half of that in a high viscous system of 60 000 mPa·s. It makes clear a linear scaling of the non-dimensional breakup time and the outer phase viscosity,  $t^* \sim \mu_o$ . This finding is consistent with the classical hydrodynamic instability of liquid jet  $t_2 = \mu_o d_{in}/\sigma$ .<sup>11</sup> The relationship can be fitted as  $t^* \sim 9.37 \times 10^{-6} \mu_o$ . It can be concluded that high viscosity is helpful for extending the unstable breakup dynamics.

#### IV. CONCLUSIONS

The breakup dynamics of toroidal droplets in immiscible viscous oils have been numerically investigated. We proposed a 2D model, taking the level-set method to accurately track the evolutions of the free interfaces. It is highlighted that the initial aspect ratios, interfacial tensions, and outer liquid viscosities play important roles in determining the breakup dynamics of toroidal droplets. The initial aspect ratios dominate the number of split droplets, which is consistent with a linearly scaling law  $n = 0.57R_0/a_0$  in the previous experiments. By considering the key factors of interfacial tension in this process, we found that interfacial tension plays a crucial role in the initial morphology of the toroidal droplet and helps to retard the unstable breakup dynamics. Interestingly, reducing the interfacial tension could stabilize it against breakup, which leads to a inhibit breakage role. We further study the effect of viscosity on the breakup dynamics, and the competition between two relevant stresses of interfacial stress and viscous stress results in a breakup. It could be concluded that the surrounding viscous oils contribute to stabilizing the interfacial-tension-driven instabilities and

extending the breakup time. Thus, for a toroidal droplet in high viscosity oils and a sufficiently low interfacial tension system, the unstable breakup dynamics could be delayed. Our findings provide a novel fundamental understanding of toroidal droplets and should be beneficial to any applications involving the manipulation of toroidal droplets.

## ACKNOWLEDGMENTS

This work was supported by the National Natural Science Foundation of China (Grant No. 12162011), Guangxi Science and Technology Project (Grant No. ZY20198017), Young Elite Scientists Sponsorship Program by CAST (Grant No. 2021QNRC001), and the Guangxi Key Laboratory of Manufacturing System and Advanced Manufacturing Technology (Grant No. 22-35-4-S011).

## AUTHOR DECLARATIONS

### Conflict of Interest

The authors have no conflicts to disclose.

## Author Contributions

**Shiyi Qin:** Investigation (equal); Writing – original draft (equal). **Zhaolin Li:** Investigation (equal). **Xun Wang:** Conceptualization (equal); Methodology (equal); Supervision (equal). **Kai Li:** Conceptualization (equal); Methodology (equal); Supervision (equal). **Xue Chen:** Conceptualization (equal); Methodology (equal); Writing – review & editing (equal).

## DATA AVAILABILITY

The data that support the findings of this study are available within the article.

## REFERENCES

- J. Plateau, "I. Experimental and theoretical researches on the figures of equilibrium of a liquid mass withdrawn from the action of gravity—Third series," *London, Edinburgh, Dublin Philos. Mag. J. Sci.* **14**(90), 1–22 (1857).
- J. D. McGraw, J. Li, D. L. Tran, A.-C. Shi, and K. Dalnoki-Veress, "Plateau-Rayleigh instability in a torus: Formation and breakup of a polymer ring," *Soft Matter* **6**, 1258–1262 (2010).
- J. Eggers and E. Villermaux, "Physics of liquid jets," *Rep. Prog. Phys.* **71**, 036601 (2008).
- E. Villermaux and B. Bossa, "Single-drop fragmentation determines size distribution of raindrops," *Nat. Phys.* **5**(9), 697–702 (2009).
- K. Marten, K. Shariff, S. Psarakos, D. J. White, and M. Merriam, "Ring bubbles of dolphins," *Sci. Am.* **275**(2), 82–87 (1996).
- Y. Wu, J. D. Fowlkes, N. A. Roberts, J. A. Diez, L. Kondic, A. G. González, and P. D. Rack, "Competing liquid phase instabilities during pulsed laser induced self-assembly of copper rings into ordered nanoparticle arrays on SiO<sub>2</sub>," *Langmuir* **27**(21), 13314–13323 (2011).
- S. Kumar, A. Ghosh, J. Chaudhuri, S. Timung, A. K. Dasmahapatra, and D. Bandyopadhyay, "Self-organized spreading of droplets to fluid toroids," *J. Colloid Interface Sci.* **578**, 738–748 (2020).
- Y.-W. Chang, A. A. Fragkopoulou, S. M. Marquez, H. D. Kim, T. E. Angelini, and A. Fernández-Nieves, "Biofilm formation in geometries with different surface curvature and oxygen availability," *New J. Phys.* **17**(3), 033017 (2015).
- M. Kojima, E. J. Hinch, and A. Acrivos, "The formation and expansion of a toroidal drop moving in a viscous fluid," *Phys. Fluids* **27**(1), 19–32 (1984).
- A. Banerjee, O. M. Lavrenteva, I. Smagin, and A. Nir, "Viscoplastic toroidal drop in compressional Stokes flow," *Phys. Fluids* **33**, 073101 (2021).
- E. Paim and A. Fernández-Nieves, "Generation and stability of toroidal droplets in a viscous liquid," *Phys. Rev. Lett.* **102**(23), 234501 (2009).
- R. F. Engberg and E. Y. Kenig, "Numerical simulation of rising droplets in liquid–liquid systems: A comparison of continuous and sharp interfacial force models," *Int. J. Heat Fluid Flow* **50**, 16–26 (2014).
- Z. Yao and M. J. Bowick, "The shrinking instability of toroidal liquid droplets in the Stokes flow regime," *Eur. Phys. J. E* **34**(3), 32 (2011).
- A. A. Fragkopoulou, E. Paim, E. Berger, P. N. Segre, and A. Fernández-Nieves, "Shrinking instability of toroidal droplets," *Proc. Natl. Acad. Sci. U. S. A.* **114**(11), 2871–2875 (2017).
- S. Osher and J. A. Sethian, "Fronts propagating with curvature-dependent speed: Algorithms based on Hamilton-Jacobi formulations," *J. Comput. Phys.* **79**(1), 12–49 (1988).
- M. Zabarankin, O. M. Lavrenteva, and A. Nir, "Liquid toroidal drop in compressional Stokes flow," *J. Fluid Mech.* **785**, 372–400 (2015).
- M. Zabarankin, "Liquid toroidal drop in compressional flow with arbitrary drop-to-ambient fluid viscosity ratio," *Proc. R. Soc. A* **472**(2187), 20150737 (2016).
- S. Zhao and J. Tao, "Weakly nonlinear instabilities of a liquid ring," *Phys. Fluids* **28**(11), 114104 (2016).
- H. Mehrabian and J. J. Feng, "Capillary breakup of a liquid torus," *J. Fluid Mech.* **717**(2), 281–292 (2013).
- A. G. González, J. A. Diez, and L. Kondic, "Stability of a liquid ring on a substrate," *J. Fluid Mech.* **718**(12), 246–279 (2013).
- S. Zhao and J. Tao, "Instability of a rotating liquid ring," *Phys. Rev. E* **88**(3), 033016 (2013).
- B. Song and J. Springer, "Determination of interfacial tension from the profile of a pendant drop using computer-aided image processing: 2. Experimental," *J. Colloid Interface Sci.* **184**(1), 77–91 (1996).
- L.-M. Zheng, Q.-R. Xie, X.-K. Chen, W. Zhang, R. Liu, and X. Chen, "Effects of interfacial tension on the stability of toroidal droplets in viscous oils," in *2020 7th International Forum on Electrical Engineering and Automation (IFEAA)* (IEEE, China, 2020), pp. 191–195.
- J.-J. Xu and W. Ren, "A level-set method for two-phase flows with moving contact line and insoluble surfactant," *J. Comput. Phys.* **263**, 71–90 (2014).
- O. Ghazian, K. Adamiak, and G. S. P. Castle, "Numerical simulation of electrically deformed droplets less conductive than ambient fluid," *Colloids Surf., A* **423**, 27–34 (2013).
- S. Tomotika, "On the instability of a cylindrical thread of a viscous liquid surrounded by another viscous fluid," *Proc. R. Soc. London, Ser. A* **150**, 322 (1935).